Journal of Molecular Graphics and Modelling 46 (2013) 125–131

Contents lists available at ScienceDirect

Journal of Molecular Graphics and Modelling

journal homepage: www.elsevier.com/locate/JMGM

Virtual screening of novel reversible inhibitors for marine alkaline protease MP

Xiaofeng Ji [1], Yuan Zheng [1], Wei Wang, Jun Sheng, Jianhua Hao, Mi Sun *

Yellow Sea Fisheries Research Institute, Chinese Academy of Fishery Sciences, Key Laboratory for Sustainable Utilization of Marine Fisheries Resources, Ministry of Agriculture, Qingdao Key Laboratory of Marine Enzyme Engineering, Qingdao 266071, China

ARTICLE INFO

Article history:
Received 2 July 2013
Received in revised form
12 September 2013
Accepted 9 October 2013
Available online 18 October 2013

Keywords:
Marine alkaline protease
Reversible inhibitor
Virtual screening

ABSTRACT

Marine alkaline protease (MP,[2] accession no. ACY25898) is produced by a marine bacterium strain isolated from Yellow Sea sediment in China. Previous research has shown that this protease is a cold-adapted enzyme with antioxidant activity that could be used as a detergent additive. Owing to its instability in the liquid state, MP's application in liquid detergents was limited. Therefore, the discovery of reversible MP inhibitors to stabilize the protease was imperative. Here, we used the X-ray structure of MP and recompiled AutoDock 4.2 with refined Zn^{2+} characters to screen the free chemical database ZINC. After completing the docking procedure, we applied strategies including the "initial filter", consensus scoring and pharmacophore model to accelerate the process and improve the virtual screening success rate. The "initial filter" was built based on the docking results of boronic acid derivatives validated as reversible inhibitors of MP by our previous studies. Finally, ten compounds were purchased or synthetized to test their binding affinity for MP. Three of the compounds could reversibly inhibit MP with apparent K_i values of 0.8–1.2 mmol. These active compounds and their binding modes provide useful information for understanding the molecular mechanism of reversible MP inhibition. The results may also serve as the foundation for further screening and design of reversible MP inhibitors.

1. Introduction

Proteases are enzymes that can cleave a protein into peptides by breaking the peptide bonds between the amino acids of proteins. Many enzymes secreted by extreme microbes, including cold-adapted enzymes, have evolved to function in their respective extreme environment [1,2]. Cold-adapted enzymes represent one of the largest groups of industrial enzymes with a wide range of applications in detergent, leather, food, and pharmaceutical industries, as well as in bioremediation processes [3]. The use of these enzymes in power detergents can greatly reduce the effect of phosphorus on the environment. However, proteases are always instable in the liquid state because of self-hydrolysis. As a result, it is difficult maintain protease activity as an additive to liquids, especially in enzyme-containing liquid detergents. Previous efforts have attempted to improve the storage stability of enzymes by adding protease inhibitors [4–6].

Boric acid and boronic acid derivatives are known to reversibly inhibit proteolysis enzymes. These inhibitions are reversible upon dilution, such as when a laundry detergent containing the enzyme is dissolved in the laundry wash water [7]. In the patent of Novozymes [8–10], a series of compounds containing boron were used as reversible protease inhibitors to stabilize the liquid detergent system. However, the reversible inhibitors were primarily boron-containing compounds and were identified by experimental method. Experimental limitations, such as expense and time, inhibit the speed of inhibitor discovery. Computational chemistry, in particular virtual screening, is a useful tool for inhibitor discovery. Through its use of computer-based methods to discover new ligands based on biological structures and chemical databases, virtual screening is one of the most powerful approaches to discover non-covalent inhibitors [11].

Marine alkaline protease (MP, accession no. ACY25898) is a 49-kD zinc metalloprotease that consists of 480 amino acid residues and belongs to the serralysin family. It exhibits maximal activity at 30 °C, stability at pH values between 8 and 11, and insensitivity to phenylmethanesulfonyl fluoride. Its crystal structure (PDB ID 3U1R) was solved with 2.0 Å resolutions. The structure analysis revealed that MP consisted of a two-domain structure with an N-terminus (residues 37–264) that contains the proteolysis domain and a C-terminal domain (residues 265–480) for stability. In the catalytic center, Zn^{2+} was bound to the side-chains of HIS186, HIS190, HIS196, and TYR 226 as well as a water molecule. Moreover, the water molecule was also bound to the side-chain of GLU187

* Corresponding author. Tel.: +86 53285819525; fax: +86 53285819525.
E-mail address: sunmi@ysfri.ac.cn (M. Sun).
[1] These authors contributed equally to this work.
[2] MP: the marine alkaline protease, PDB id: 3U1R.

1093-3263/$ – see front matter © 2013 Published by Elsevier Inc.
http://dx.doi.org/10.1016/j.jmgm.2013.10.004

Table 1
The experimental K_i and docking K_i and E_i values for boric acid and boronic acid derivatives.

Compounds	K_i (mM)	Docking K_i (μM)	Docking E_i (kcal/mol)
Boric acid	2.03 ± 0.040	1210	−3.98
4-Formyl-phenyl-boronic acid	0.57 ± 0.027	166.13	−5.16
Thiophene-3-boronic acid	0.81 ± 0.034	171.23	−5.14
3-Acetamidophenyl boronic acid	0.07 ± 0.003	17.69	−6.48
4-Methylthiophene-2-boronic acid	0.94 ± 0.040	108.64	−5.41
5-Ethylthiophene-2-boronic acid	0.21 ± 0.010	76.2	−5.62
5-Bromothiophene-2-boronic acid	0.27 ± 0.008	87.63	−5.54
Dibenzothiophene-1-boronic acid	0.026 ± 0.001	5.42	−7.18
Dibenzofuran-4-boronic acid	0.24 ± 0.009	67.17	−5.69
Furan-2-boronic	1.48 ± 0.053	302.45	−4.8
Furan-3-boronic	1.81 ± 0.089	526.24	−4.47
3-Methoxythiophene-2-boronic acid	0.40 ± 0.022	73.08	−5.64
5-*n*-Propylthiophene-2-boronic acid	0.07 ± 0.003	16.36	−6.53
3-Bromothiophene-boronic acid	1.16 ± 0.038	198.86	−5.05
3-Bromothiophene-4-boronic acid	0.16 ± 0.007	39	−6.01
5-Ethylfuran-2-boronic acid	0.39 ± 0.020	88.5	−5.53
Diphenyl borinic acid	0.06 ± 0.002	14.5	−6.6
5-Methoxyfuran-2-boronic acid	0.98 ± 0.033	189.67	−5.08

and TYR226. In addition, there were eight calcium ions in the MP molecule. Our previous studies indicated that some boronic acid derivatives could reversibly inhibit the activity of MP.

In the present study, we used database screening and biological evaluation to identify reversible, non-covalent inhibitors of MP. Our virtual screening approach was based on initial high throughput docking calculations performed on a library of approximately 19,000,000 commercially available compounds in the ZINC [12,13] database. The optimized zinc parameters (zinc radius: 0.87 Å; well depth: 0.35 kcal/mol; and zinc charges: +0.95e) [14,15], consensus score, and special filter strategy constructed from the experimental and docking results of boronic acid derivatives were applied to improve the success rate of reversible inhibitor identification. Ten compounds were synthesized and assayed in vitro. Three of these compounds inhibited MP with apparent K_i values of 0.8–1.2 mM and could be used for additional mechanistic characterization. This finding may provide useful information for mechanistic understanding and serve as the basis for further selection and synthesis of more effective MP inhibitors.

2. Material and methods

2.1. Generating the "flexible model" of MP for docking

In the crystal structure of MP, a flexible loop (237–243) called the "flap" hinders the substrate entrance to the active site [16]. Considering the conformational flexibility of this loop, a 10 ns implicit solution molecular dynamic (MD) simulation was performed using the Amber 11 software package and the all-atom ff03 force field [17,18]. The preparation details and production phases of the MD simulation were previously published [19] and are briefly described here. The starting model was derived from the crystal structure of MP (PDB: 3U1R). The active site zinc ion and one crystal water (HOH 801) were conserved in the model. All of the Ca^{2+} ions and the other crystal water molecules were deleted. The initial models were solvated in explicit water with the TIP3P water molecule of 10 Å layers using the LEaP module integrated in the AMBER11 package. To neutralize the redundant charges, 11 Ca^{2+} ions were added to the system. Then, the system was subjected to a two-step minimization. First, the water and metal ions were minimized with 7500 steps (2500 steps of steepest descent followed by 5000 steps of conjugate gradient) where the atomic positions of the solute were initially restrained using a harmonic potential. Next, the whole system was minimized with 7500 steps (2000 steps of steepest descent followed by 5000 steps of conjugate gradient). Non-bonded interactions were calculated using a cutoff distance of 12 Å with the Particle Mesh Ewald (PME) method under periodic boundary conditions [20]. The minimization was followed by a slow heating from 0 to 300 K over a period of 200 ps using the Langevin thermostat [21] with a collision frequency of 2 ps^{-1}. The heating process was performed with the NVT ensemble under periodic boundary conditions, and the atomic positions of MP were restrained. Then, a total of 20 ns simulations were performed at constant temperature (300 K) and pressure (1 bar) using the Berendsen algorithm [22] with a coupling constant of 1.0 ps for both parameters. All bonds involving hydrogen atoms were constrained with the SHAKE algorithm [23]. The Ptraj module was used for the analysis of trajectories and the root mean square deviation (RMSD) was calculated for the protein backbone atoms (C_α). The simulation achieved equilibrium after 13 ns. After equilibration, structures from each 1 ps interval were selected and finally a total of 7000 structures were selected. These selected structures were clustered with a RMSD threshold of 1.5 Å. The clustering algorithm used was based on a pairwise method by Daura et al. [24], and the Ca atoms of the two flaps (T237-A244 and S140-A147) were exclusively considered. After the conformation clustering, two major groups of the structures can be used for further docking studies. One confirmation group was similar to the original structure with a closed loop conformation and a small binding site, whereas the other group contained a loop that flipped away from the active site and a larger binding site.

In the open conformations group (loops flip away from the active site), we calculated the distance between flap1 and flap2 for each conformation. Structures with the farthest, shortest and most neutral distances were selected and named S1, S2 and S3, respectively. We docked the boric and boronic acid derivatives to the three structures. The results suggested that the corresponding theoretical docking E_i and K_i values did not change dramatically with different receptor conformations as only slight differences (no greater than 0.5) were observed. This result may be attributed to reduced discrimination between conformations in the open cluster. Structures with an RMSD of 1.5 Å were considered similar. Furthermore, the binding sites were set as flexible during the docking procedure. Hence, the conformation should not significantly influence the result. In this manuscript, we selected S2, with the largest active pocket, as the initial structure for further docking studies.

2.2. Docking studies and the "initial filter" building

MP (PDBid: 3U1R) was defined as the acceptor, and the heteroatoms including the water molecules and Ca^{2+} ions were

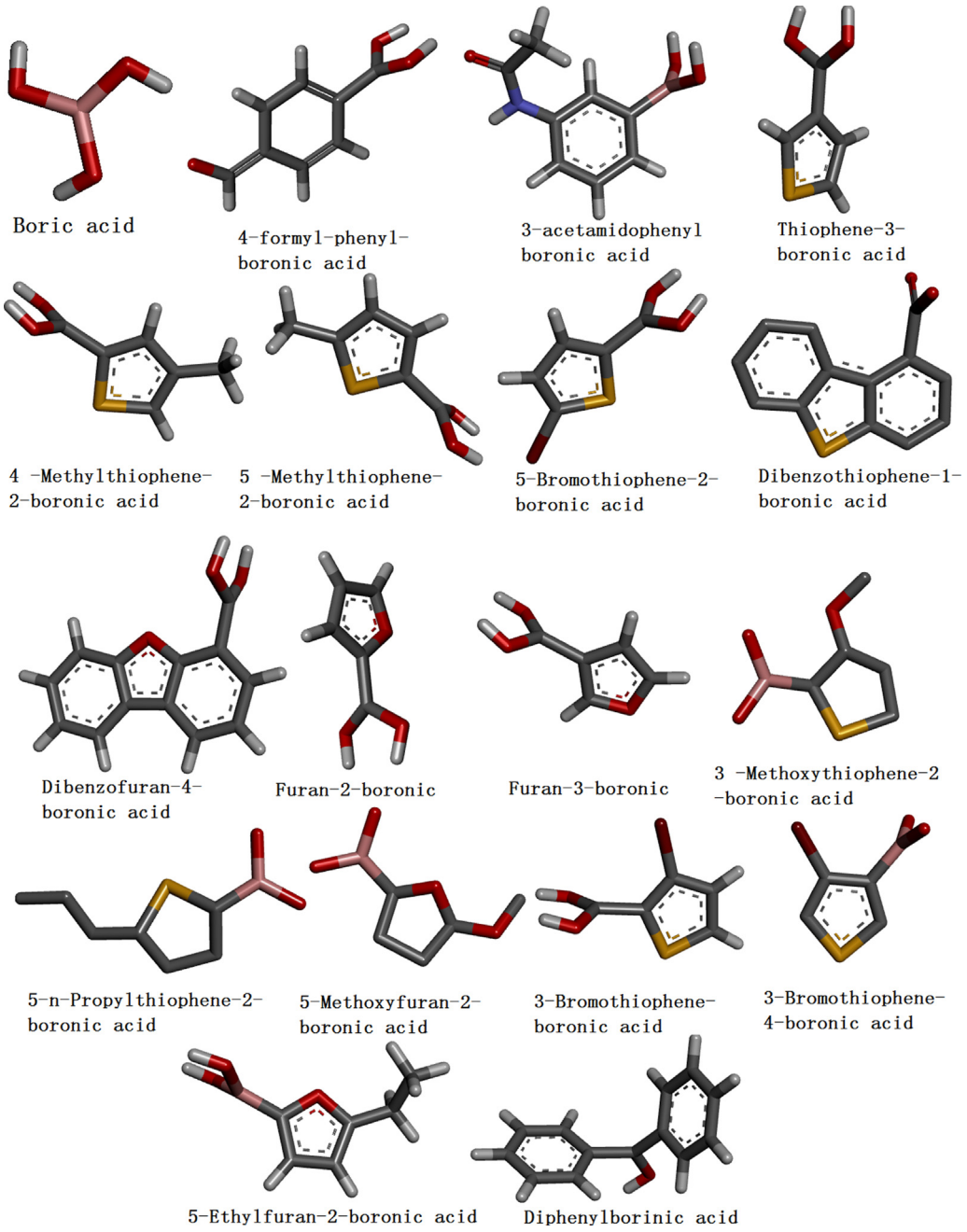

Fig. 1. Chemical structures of boric acid and its derivations.

removed. The zinc ion at the active site was retained. The active site was defined using AutoGrid, and the center (12.994, −17.897, 27.715) of the box was chosen according to the position of a key residue in pocket. The grid size was set to 90 × 90 × 90 points with grid spacing of 5 Å. The grid box included the entire binding site of the enzyme, and the residues in active site were set as flexible for the whole docking process. For each independent run, the operator weights for crossover, mutation, and elitism were set as default parameters (0.80, 0.02, and 1, respectively). Small molecules were defined as ligands. The procedure was performed considering the flexibility of the ligand, i.e., all rotational bonds were set free. A short minimization (100 steepest descent steps using Amber force fields with a gradient convergence value of 0.05 kcal/mol Å) was performed to release any internal strain.

The AutoDock 4.2 program is a proven robust approach with good docking accuracy and reliability for metalloproteinase inhibitors [14,15]. In this work, a recompiled AutoDock program with optimized Zn^{2+} parameters was employed for docking calculations. AutoDock Tools (ADT) [25] was used to prepare molecules, and all of the hydrogen was added by using REDUCE [26]. All of the docking decoys were clustered with an RMSD cutoff value of 2 Å.

Boric acid and boronic acid derivatives are known to reversibly inhibit proteolytic enzymes [27–29]. Our previous studies of reversible MP inhibitors revealed that some boronic acid derivatives are good reversible inhibitors (Table 1). Hence, we used these compounds to train the characters and built an "initial filter" for the virtual screen. All of the character settings followed the steps mentioned above. The tertiary structure of the boric acid and boronic acid derivatives were listed in Fig. 1. These structures were downloaded from Chemspider [30] (http://www.chemspider.com/). Although the following compounds had strong inhibition ability,

they were not reversible inhibitors of MP: dibenzothiophene-1-boronic acid, 3-acetamidophenyl boronic acid, diphenyl borinic acid, 3-bromothiophene-4-boronic acid and 5-n-propylthiophene-2-boronic acid. In addition, boric acid (BC) was also not an effective reversible inhibitor of MP with a K_i value 2.03 ± 0.040 mM. The lack of inhibitory activity could be attributed to the fact that the MP-BC complex was not stable and the inhibitor (BA) fell off the complex. Similar to BA, furan-2-boronic and furan-3-boronic also had weak binding affinities with K_i values of 1.48 ± 0.053 mM and 1.81 ± 0.089 mM, respectively. These results demonstrate that the three compounds were not effective inhibitors of MP. We docked these compounds to MP using the AutoDock 4.2 software. The E_i and K_i docking values of the favorite clusters were extracted and listed in Table 1. Considering the above factors, the "initial filter" for MP reversible inhibitor selection was set using the following parameters: a docking E_i value between −6.00 and −5.00 kcal/mol and a docking K_i value between 50 and 200 μM.

2.3. Virtual docking screen combined with consensus scoring and "initial filter"

Approximately 19,000,000 commercially available compounds from the free database ZINC were used as the docking library. The tertiary structures of the compounds included in the docking library were downloaded from the ZINC database. Virtual screening with docking was performed with a Linux Cluster Platform. We chose compounds for our primary selection list based on the selective criteria for both dock energy scores and K_i scores ($-6.000 \le E_i \le -5.000$; $50 \le K_i \le 200$). After this filter, approximately 13,000 compounds were selected.

Following the "initial filter" screening, the X-score [31] program, which computes the binding affinity for a given ligand molecule to its target protein, was applied to reevaluate the primary selected molecules. The calculated score could potentially remove the score bias caused by single docking and was considered more accurate and representative of the actual binding ability. Multiple conformations of the 13,000 compounds were then calculated and reevaluated by X-score to generate the final "hit lists". All compounds with scores greater than 5.0 and docking E_i and X-scores ranked among the top 2000 remained in the hits list. Finally, 283 compounds were selected.

To further refine our hits list, a visual inspection was performed. Based on the structure of active site, a pharmacophore model (Fig. 2) was generated using the LigGuilderV2 cavity module [32]. We applied this pharmacophore model to select the final compounds from the remaining 283 candidates. The molecules that best matched the pharmocophore were retained. Compounds that did not match sufficient pharmacophore elements or possessed more than double the elements were removed from the candidate lists.

2.4. Protease assay

2.4.1. Enzyme purification

MP was purified by ultrafiltration membrane and Superdex 200 gel filtration chromatograph according to the methods of Zhang et al. [16]. During the purification, the protease activities were spectrophotometrically assayed by the azocasein (Sigma) method.

Protease activity was assayed at 30 °C using azocasein as a substrate. The assay mixture contained 400 μL of 0.1 mol/l Tris-HCl buffer (pH 9), 250 μL of the enzyme sample, and 100 μL of 1% (w/v) azocasein. TCA was added to stop the reaction. The activity was estimated spectrophotometrically by reading the absorbance at 345 nm. In this assay, one enzyme unit was expressed as the amount of enzyme that caused an increase of 0.01 in the absorbance at 345 nm per minute [33]. Analysis of the samples during protein purification was performed using SDS-PAGE [34]. Protein

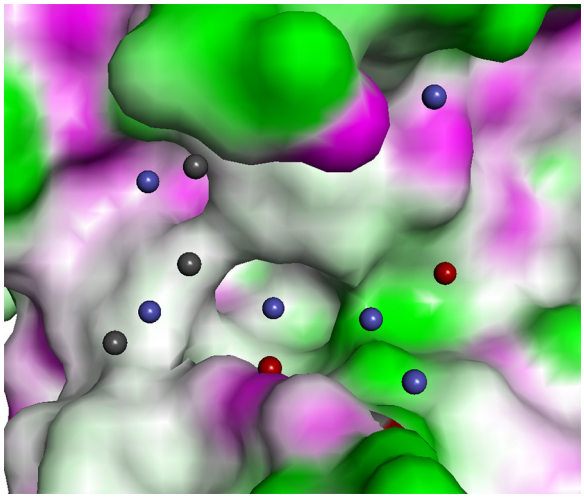

Fig. 2. The pharmacophore model generated by the cavity module from LigBuilder V2 based on the active site structure of MP. Red, blue and black balls represent hydrogen bond acceptor, hydrogen bond donor and hydrophobic sites, respectively. The figure was generated by Discovery 3.0 Client and shown as the solvent hydrogen donor/acceptor surface. (For interpretation of the references to color in this figure legend, the reader is referred to the web version of this article.)

concentrations were estimated by measuring the absorbance at 280 nm and using a protein-dye binding assay [35]. The purified marine protease was lyophilized.

2.4.2. Inhibitors

The effect of inhibitors on MP activity was studied at 30°Cusing Succ-Ala-Ala-Pro-Arg-AMC as a substrate. The enzyme was pre-incubated with the inhibitors for 5 min. The measurements were performed in a final volume of 200 μL enzyme assay buffer (50 mM Tris–HCl (pH 8.0), 10 mM $CaCl_2$, 0.1 M NaCl) at 30 °C with 5–30 ng/mL enzyme. The activities on the fluorometric substrates were measured at 380 nm excitation and 460 nm emission wavelengths [36]. The Michaelis constant (K_m) for MP was determined using Lineweaver–Burk plots, and the K_i value was obtained from the Dixon plots. Boric acid and its derivatives induced competitive inhibition. To describe the competitive inhibition mechanism, the Lineweaver–Burk equation in double reciprocal form can be written as:

$$\frac{1}{v_i} = \frac{K_m}{V_{max}}\left(1 + \frac{[I]}{K_i}\right)\frac{1}{[S]} + \frac{1}{V_{max}}. \quad (1)$$

Secondary plots can be constructed from

$$K_m^{app} = \frac{K_m[I]}{K_i} + K_m. \quad (2)$$

The K_i, K_m, and V_{max} values can be derived from the above equations. The secondary replot of the apparent Km vs. [I] is linearly fitted, assuming a single inhibition site or a single class of inhibition sites [37].

3. Results and discussion

The compounds isolated from the virtual screening were tested for their inhibitory effects on MP. The top ten X-score compounds (Table 2 Fig. 6) from the hits list were selected and ordered (or synthesized). Their binding affinities were measured using the assay method mentioned above. We tested the inhibition affinities for the ten compounds. Three of the selected compounds efficiently inhibited the activity of MP. The K_i values for these three compounds were experimentally determined as 0.84 ± 0.13 mM, 1.28 ± 0.055 mM, and 1.02 ± 0.044 mM

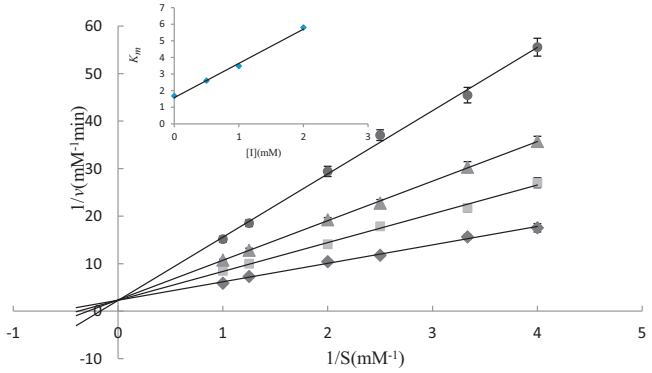

Fig. 3. Plot of $1/v$ vs. $1/[S]$. The concentrations of ZINC02961282 were 0 (–♦–), 0.50 (–■–), 1.00 (–▲–) and 2.00 (–●–) mM, respectively. The label in figure is presented as the absolute error. The inset represents the plot of K_m vs. $[I]$ used to ascertain K_i.

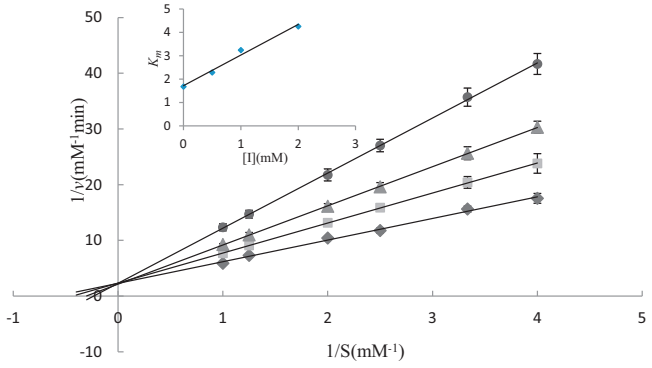

Fig. 4. Plot of $1/v$ vs. $1/[S]$. The concentrations of ZINC03025346 were 0 (–♦–), 0.50 (–■–), 1.00 (–▲–) and 2.00 (–●–) mM, respectively. The label in figure is presented as the absolute error. The inset represents the plot of K_m vs. $[I]$ used to ascertain K_i.

Table 2
Docking scores, X-scores and experimental K_i values for candidates.

Compounds	Docking energy (kcal/mol)	Docking K_i	X-score	K_i (mmol)
ZINC00344328	168.04	−5.15	6.87	
ZINC20476815	124.22	−5.33	6.36	
ZINC02961282	101.33	−5.45	6.21	0.84 ± 0.13
ZINC19908801	197.07	−5.06	5.88	
ZINC03025346	163.75	−5.16	5.87	1.28 ± 0.055
ZINC02108418	160.56	−5.18	5.87	
ZINC00832337	193.56	−5.07	5.63	
ZINC01006243	162.44	−5.17	4.8	1.02 ± 0.044
ZINC04018940	141.88	−5.25	4.8	
ZINC02064260	123.83	−5.33	4.73	

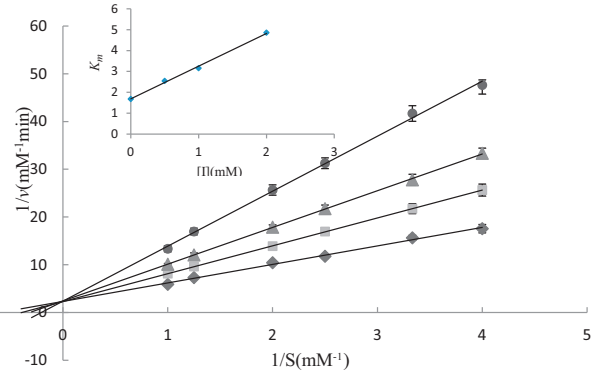

Fig. 5. Plot of $1/v$ vs. $1/[S]$. The concentrations of ZINC01006243 were 0 (–♦–), 0.50 (–■–), 1.00 (–▲–) and 2.00 (–●–) mM, respectively. The label in figure is presented as the absolute error. The inset represents the plot of K_m vs. $[I]$ used to ascertain K_i.

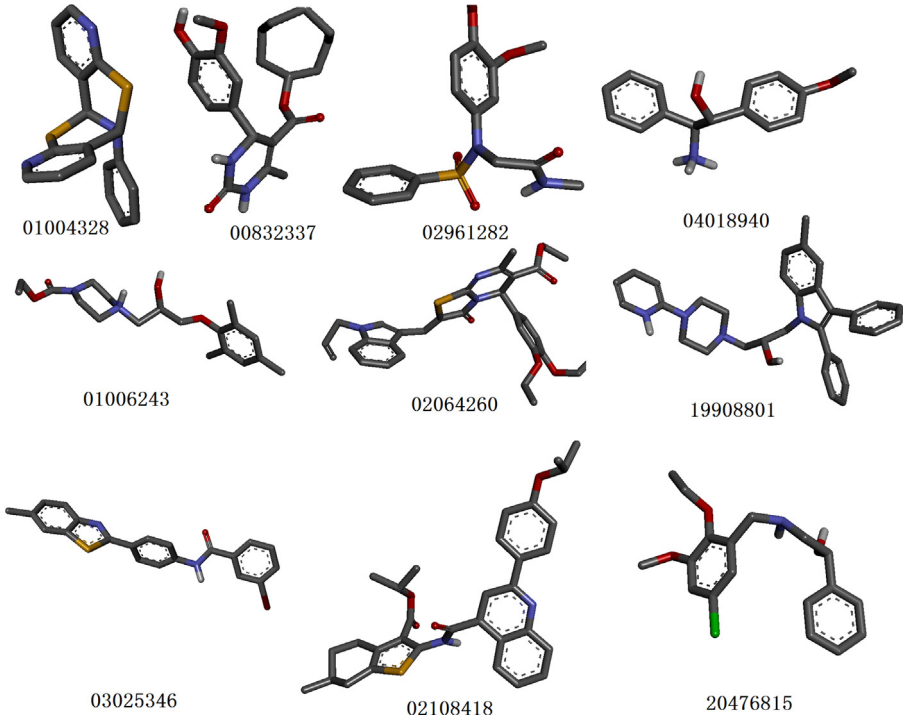

Fig. 6. The chemical structures of active compounds identified by virtual screening.

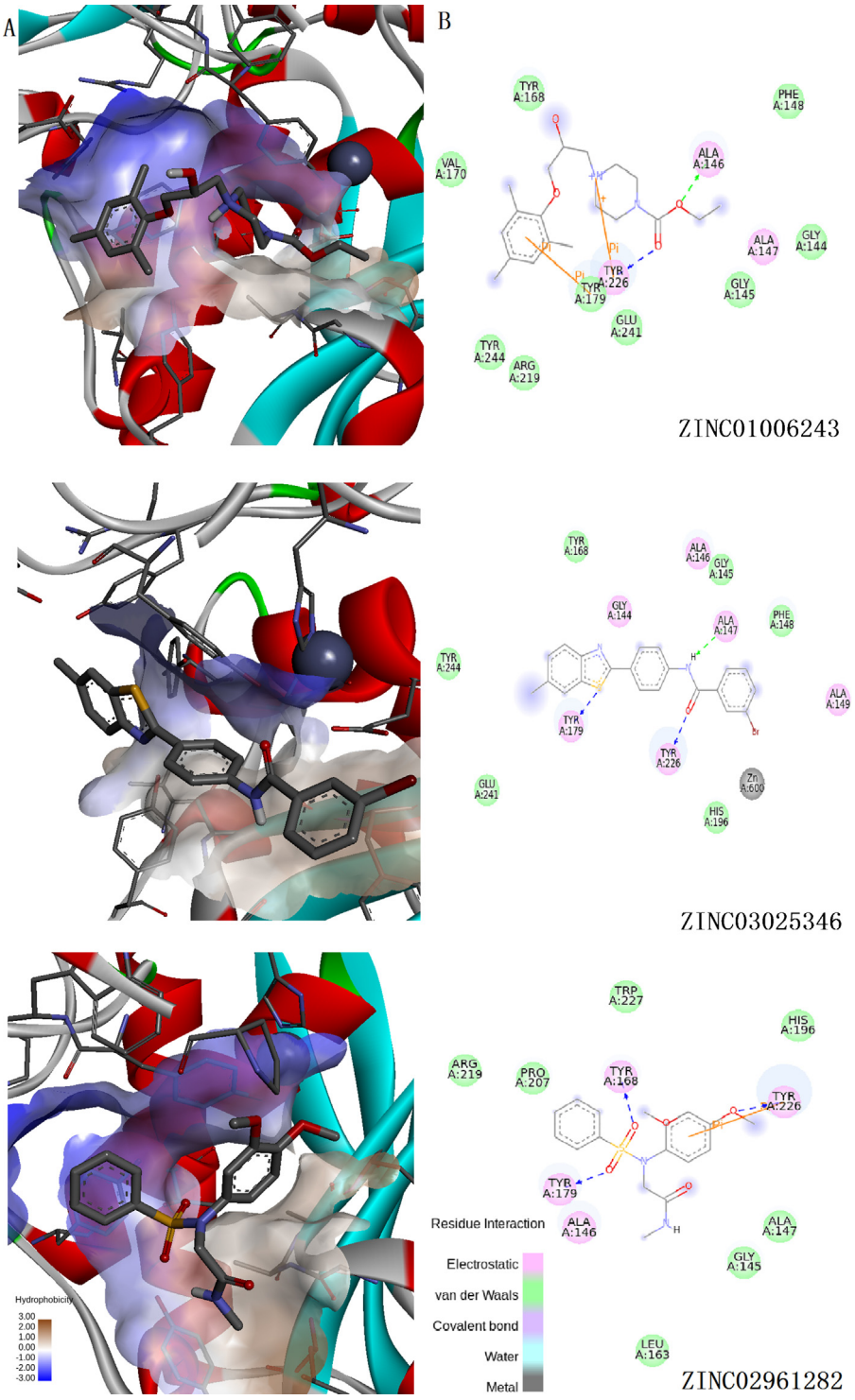

Fig. 7. The binding modes of ZINC01006243, ZINC03025346 and ZINC02961282 with MP. All of the interaction pictures were generated using Discovery 3.0 Client. The left column depicts the binding mode shown as receptor hydrophobic surfaces with ligand ball-and-stick. The right column represents the 2D diagram of the interactions between the receptor and ligand.

for compounds ZINC02961282, ZINC03025346 and 1.02 ± 0.044, respectively. These compounds were all reversible inhibitors of MP.

The enzyme kinetics in the presence of the inhibitor was studied using double-reciprocal Lineweaver–Burk plots. The results (Figs. 3–5) revealed that the V_m values remained the same and the K_m values increased with increasing inhibitor concentrations, indicating that the selected compounds induced competitive inhibition. The K_i values were calculated using Eqs. (1) and (2). Under the conditions employed in the present study, MP-induced hydrolysis follows Michaelis–Menten kinetics. The kinetic parameters for the enzyme were obtained from the Lineweaver–Burk plots (Figs. 3–5, curve –♦–), and the results show that the K_m and V_m are 1.68 ± 0.13 mM and 0.43 ± 0.051 mM/min, respectively.

Three molecules were determined to reversibly inhibit MP: ZINC02961282, ZINC03025346 and ZINC01006243. The K_i values of these compounds ranged from 0.8 to 1.2 mM. Next, we wanted

to determine how these compounds bind to MP. To elucidate the inhibitory mechanism at the molecular level, we re-docked these compounds to MP. The binding pose for the three compounds determined by AutoDock 4.2 is shown in Fig. 7. As shown in Fig. 7, all of the three compounds form interactions with TYR226 and TYR179. With regard to ZINC01006243, the benzene ring forms a Pi-Pi interaction with TYR179. Moreover, N2 and TYR226 form a cation Pi interaction, and TYR226 and O2 are hydrogen-bonded. The main chain of ALA146 serves as the electron donor to form a hydrogen bond interaction with ZINC01006243. The interaction between ZINC03025346 and MP is primarily hydrogen-bond interactions between S1, H11, O1 and TYR179, TYR226 and ALA147, respectively. Similar to the interaction between ZINC01006243 and MP, the benzene ring in ZINC02961282 also forms a Pi–Pi interaction with TYR226 in MP. Meanwhile, the side chain of TYR226 forms a hydrogen bond interaction with O_3.

4. Conclusions

After the virtual docking screen and post-dock scoring filters, ten potential compounds were selected and purchased for biological testing. Three of the compounds were found to reversibly inhibit MP in the millimolar range. These active compounds served as the basis for developing MP inhibitors. The binding conformation of the active compounds also provides useful clues for identifying and optimizing MP inhibitors. Overall, our results further demonstrate the effectiveness of the automated AutoDock program with the improved scoring function as a docking program for the de novo discovery of inhibitors. It is also useful for binding mode analysis to elucidate the activities of the identified inhibitors. The three novel inhibitors of MP identified in this study are expected to serve as new starting points in the development of more potent MP inhibitors.

Acknowledgements

The authors are grateful to Professor Yi Xiao and associate Professor Shiyong Liu, the college of theoretical biology, Huazhong University of Science and Technology for the guidelines on theoretical analysis. This work is supported by the Specific International Cooperation and Exchanges in Science and Technology (2011DFB30250), the National High Technology Research and Development Program ("863" Program) of China (2011AA090703) and Special Scientific Research Funds for Central Non-profit Institutes, Yellow Sea Fisheries Research Institutes (Nos. 20603022013029 and 20603022013030).

References

[1] L. Loperena, V. Soria, H. Varela, S. Lupo, A. Bergalli, M. Guigou, A. Pellegrino, A. Bernardo, A. Calvino, F. Rivas, S. Batista, Extracellular enzymes produced by microorganisms isolated from maritime Antarctica, World J. Microbiol. Biotechnol. 28 (2012) 2249–2256.
[2] J.C. Marx, T. Collins, S. D'Amico, G. Feller, C. Gerday, Cold-adapted enzymes from marine Antarctic microorganisms, Mar. Biotechnol. (NY) 9 (2007) 293–304.
[3] R. Gupta, Q.K. Beg, P. Lorenz, Bacterial alkaline proteases: molecular approaches and industrial applications, Appl. Microbiol. Biotechnol. 59 (2002) 15–32.
[4] A. Svendsen, I.G. Clausen, et al., Detergent compositions containing protease and novel inhibitors for use therein, United States Patent 5674833, 1997.
[5] P. Schulz, K. Schwadtke, E. Smulders, Process for the preparation of a storage-stable liquid detergent composition, United States Patents US4929380 A, 1990.
[6] M.R. Stoner, D.A. Dale, P.J. Gualfetti, T. Becker, M.C. Manning, J.F. Carpenter, T.W. Randolph, Protease autolysis in heavy-duty liquid detergent formulations: effects of thermodynamic stabilizers and protease inhibitors, Enzyme Microb. Technol. 34 (2004) 114–125.
[7] R.K. Panandiker, D.W. Bjorkquist, Liquid detergents with ortho-substituted phenylboronic acids for inhibition of proteolytic enzyme (1995).
[8] R.G. Severson Jr., Liquid detergents containing boric acid and formate to stabilize enzymes, U.S. Patent 4,537,707, 1985.
[9] L.K. Nielsen, A. Deane-Wray, Boronic acid or borinic acid derivatives as enzyme stabilizers, WO Patent 1,995,002,046, 1999.
[10] L.K. Nielsen, A. Deane-Wray, 4-Substituted-phenyl-boronic acids as enzyme stabilizers, EP0832174 B1, 1999.
[11] G. Schneider, Virtual screening: an endless staircase? Nat. Rev. Drug Discov. 9 (2010) 273–276.
[12] J.J. Irwin, B.K. Shoichet, ZINC – a free database of commercially available compounds for virtual screening, J. Chem. Inf. Model. 45 (2005) 177–182.
[13] J.J. Irwin, T. Sterling, M.M. Mysinger, E.S. Bolstad, R.G. Coleman, ZINC:, A free tool to discover chemistry for biology, J. Chem. Inf. Model. 52 (2012) 1757–1768.
[14] X. Hu, W.H. Shelver, Docking studies of matrix metalloproteinase inhibitors: zinc parameter optimization to improve the binding free energy prediction, J. Mol. Graph. Model. 22 (2003) 115–126.
[15] X. Hu, S. Balaz, W.H. Shelver, A practical approach to docking of zinc metalloproteinase inhibitors, J. Mol. Graph. Model. 22 (2004) 293–307.
[16] S.C. Zhang, M. Sun, T. Li, Q.H. Wang, J.H. Hao, Y. Han, X.J. Hu, M. Zhou, S.X. Lin, Structure analysis of a new psychrophilic marine protease, PLoS ONE 6 (2011) e26939.
[17] D. Case, D. TA, C. TE III, S. CL, AMBER 11, University of California, San Francisco, 2010.
[18] Y. Duan, C. Wu, S. Chowdhury, M.C. Lee, G. Xiong, W. Zhang, R. Yang, P. Cieplak, R. Luo, T. Lee, A point-charge force field for molecular mechanics simulations of proteins based on condensed-phase quantum mechanical calculations, J. Comput. Chem. 24 (2003) 1999–2012.
[19] X. Ji, W. Wang, Y. Zheng, J. Hao, M. Sun, Homology modeling and molecular dynamics simulation studies of a marine alkaline protease, Bioinform. Biol. Insights 6 (2012) 255–263.
[20] U. Essmann, L. Perera, M.L. Berkowitz, T. Darden, H. Lee, L.G. Pedersen, A smooth particle mesh Ewald method, J. Chem. Phys. 103 (1995) 8577–8593.
[21] R.J. Loncharich, B.R. Brooks, R.W. Pastor, Langevin dynamics of peptides: the frictional dependence of isomerization rates of N-acetylalanyl-N′-methylamide, Biopolymers 32 (1992) 523–535.
[22] H.J. Berendsen, J.P.M. Postma, W.F. van Gunsteren, A. DiNola, J.R. Haak, Molecular dynamics with coupling to an external bath, J. Chem. Phys. 81 (1984) 3684.
[23] J. Ryckaert, G. Ciccotti, H.J. Berendsen, Numerical integration of the cartesian equations of motion of a system with constraints: molecular dynamics of *n*-alkanes, J. Comput. Phys. 23 (1977) 327–341.
[24] X. Daura, K. Gademann, B. Jaun, D. Seebach, W.F. van Gunsteren, A.E. Mark, Peptide folding: when simulation meets experiment, Angew. Chem. Int. Ed. 38 (1999) 236–240.
[25] G.M. Morris, R. Huey, W. Lindstrom, M.F. Sanner, R.K. Belew, D.S. Goodsell, A.J. Olson, AutoDock4 and AutoDockTools4: Automated docking with selective receptor flexibility, J. Comput. Chem. 30 (2009) 2785–2791.
[26] J.M. Word, S.C. Lovell, J.S. Richardson, D.C. Richardson, Asparagine and glutamine: using hydrogen atom contacts in the choice of side-chain amide orientation, J. Mol. Biol. 285 (1999) 1735–1747.
[27] R. Smoum, A. Rubinstein, V.M. Dembitsky, M. Srebnik, Boron containing compounds as protease inhibitors, Chem. Rev. 112 (2012) 4156–4220.
[28] R.N. Lindquist, C. Terry, Inhibition of subtilisin by boronic acids, potential analogs of tetrahedral reaction intermediates, Arch. Biochem. Biophys. 160 (1974) 135–144.
[29] M. Philipp, S. Maripuri, Inhibition of subtilisin by substituted arylboronic acids, FEBS Lett. 133 (1981) 36–38.
[30] H.E. Pence, A. Williams, ChemSpider: an online chemical information resource, J. Chem. Edu. 87 (2010) 1123–1124.
[31] R. Wang, Y. Lu, S. Wang, Comparative evaluation of 11 scoring functions for molecular docking, J. Med. Chem. 46 (2003) 2287–2303.
[32] Y. Yuan, J. Pei, L. Lai, LigBuilder 2: a practical de novo drug design approach, J. Chem. Inform. Model. 51 (2011) 1083–1091.
[33] F.J. Romero, L.A. Garcı′a, J.A. Salas, M. Dı′az, L.M. Quirós, Production, purification and partial characterization of two extracellular proteases from *Serratia marcescens* grown in whey, Process Biochem. 36 (2001) 507–515.
[34] U.K. Laemmli, Cleavage of structural proteins during the assembly of the head of bacteriophage T4, Nature 227 (1970) 680–685.
[35] M.M. Bradford, A rapid and sensitive method for the quantitation of microgram quantities of protein utilizing the principle of protein-dye binding, Anal. Biochem. 72 (1976) 248–254.
[36] M.K. Massaoud, J. Marokházi, I. Venekei, Enzymatic characterization of a serralysin-like metalloprotease from the entomopathogen bacterium, *Xenorhabdus*, Biochim. Biophys. Acta (BBA) – Proteins Proteom. 1814 (2011) 1333–1339.
[37] Y. Si, Z. Wang, D. Park, H.Y. Chung, S. Wang, L. Yan, J. Yang, G. Qian, S. Yin, Y. Park, Effect of hesperetin on tyrosinase: inhibition kinetics integrated computational simulation study, Int. J. Biol. Macromol. 50 (2012) 257–262.